IEICE TRANSACTIONS

on Communications

VOL. E105-B NO. 3
MARCH 2022

A PUBLICATION OF THE COMMUNICATIONS SOCIETY

The Institute of Electronics, Information and Communication Engineers
Kikai-Shinko-Kaikan Bldg., 5-8, Shibakoen 3chome, Minato-ku, TOKYO, 105-0011 JAPAN

PAPER

Specific Absorption Rate (SAR) Calculations in the Abdomen of the Human Body Caused by Smartphone at Various Tilt Angles: A Consideration of the 1950 MHz Band

Chiaki TAKASAKA[†], ***Student Member***, **Kazuyuki SAITO**[†a)], ***Member***, **Masaharu TAKAHASHI**[†], ***Fellow***, **Tomoaki NAGAOKA**[††], ***and*** **Kanako WAKE**[††], ***Members***

SUMMARY Various electromagnetic (EM) wave applications have become commonplace, and humans are frequently exposed to EM waves. Therefore, the effect of EM waves on the human body should be evaluated. In this study, we focused on the specific absorption rate (SAR) due to the EM waves emitted from smartphones, developed high-resolution numerical smartphone models, and studied the SAR variation by changing the position and tilt angle (the angle between the display of the smartphone model and horizontal plane) of the smartphone models vis-à-vis the human abdomen, assuming the use of the smartphone at various tilt angles in front of the abdomen. The calculations showed that the surface shape of the human model influenced the SAR variation.

key words: *numerical smartphone model, finite-difference time-domain (FDTD) method, specific absorption rate (SAR), dosimetry*

1. Introduction

Various electromagnetic (EM) wave applications are currently being used and have the effect of enriching our lives. The cellular phone is a typical example. In particular, smartphone use has rapidly become widespread and indispensable to our daily lives. As a result, we are frequently exposed to the EM waves emitted from these radio communication devices.

In order to evaluate the influence of EM exposure to the human body, it is important to estimate the specific absorption rate (SAR), which is the amount of power absorption per unit mass of tissue. This is expressed in the following equation:

$$\mathrm{SAR} = \frac{\sigma}{\rho} E^2 \tag{1}$$

where σ is the conductivity of the tissue (S/m), ρ is the density of the tissue (kg/m^3), and E is the root mean square of the internal electric field (V/m). In the International Commission on Non-Ionizing Radiation Protection (ICNRP) and the Institute of Electrical and Electronics Engineers (IEEE), a spatial SAR averaged over any 10 grams of tissue ($\mathrm{SAR}_{10\,\mathrm{g}}$) is used as an evaluation index of near field exposure [1], [2]. SARs in the human body are principally estimated by numerical simulation because ethical concerns make it difficult to measure the SAR in a living person's body. Heretofore, a number of studies have calculated the SAR in the human head because of the tendency to hold the phone near the head while on a call [3]–[7].

In recent years, smartphones have come to be frequently used for data communication, such as E-mail, social media, gaming, etc. As such, we hold the smartphone in front of our bodies rather than near the head. In the context of these circumstances, several studies have calculated the SAR in the human abdomen [8], [9]. Tateno et al. calculated the $\mathrm{SAR}_{10\,\mathrm{g}}$ in the human body due to exposure from flip phones and tablet computers [8]. Takei et al. developed a high-resolution numerical smartphone model [9]. They then calculated the SAR when the smartphone model was placed in front of the torso of the human model, changing the tilt angles and height of the smartphone. Here, the tilt angle is defined as the angle between the display of the smartphone model and the horizontal plane. Takei et al. found that the peak $\mathrm{SAR}_{10\,\mathrm{g}}$ varied depending on the positional relationship between the smartphone and the human model [9]. However, few studies have focused on the SAR variation caused by tilt changes to the smartphone angles or differences in the types of smartphone. It is necessary to conduct simulations using multiple smartphone models because the location of the antenna in smartphones differs based on types of smartphone.

In this study, we developed new high-resolution numerical smartphone models for highly accurate SAR evaluations and calculated the SARs under the assumption that an adult male would be holding the smartphone at various tilt angles in front of the abdomen. These analyses are of a specific model. However, by statistically analyzing the results, we considered that they could be regarded in a somewhat general sense. In addition, we investigated SAR variations by changing the tilt angles of the smartphone in three pattern surfaces on the human body.

2. Smartphone Model

2.1 Development of the Numerical Smartphone Models

The numerical smartphone model was developed on the ba-

Manuscript received March 12, 2021.
Manuscript revised July 20, 2021.
Manuscript publicized September 1, 2021.

[†]The authors are with Chiba University, Chiba-shi, 263-8522 Japan.
[††]The authors are with the National Institute of Information and Communications Technology, Koganei-shi, 184-8795 Japan.
a) E-mail: kazuyuki_saito@faculty.chiba-u.jp

DOI: 10.1587/transcom.2021EBP3040

Table 1 Electrical constants of the smartphone model.

Parts	Relative permittivity	Conductivity [S/m]
Printed circuit board (PCB)	2.0 – 5.0	0.0
Plastic case	2.2 – 4.0	0.0
Other plastic parts	1.8 – 5.0	0.0
Antenna IC (integrated circuit) Metal plate Battery	Perfect electric conductor	

sis of a commercially available smartphone. First, an actual smartphone was disassembled to determine its internal structure and measure the size of its internal parts. Second, on the basis on these data, a smartphone model was developed using computer aided design (CAD) software. Finally, the CAD model was divided into small cells, and electrical properties were allocated to each cell. It is difficult to develop a smartphone model as an EM source that acts like an actual smartphone using only a high-resolution "shape." Therefore, the electrical properties were adjusted so that the antenna would work at the operating frequency and would not be based on measuring the electrical properties of the actual internal parts. These adjustments were performed based on experience from our previous study, not at random. Table 1 summarizes the electrical constants of the parts in the smartphone models.

We developed three types of smartphone models: models A–C, respectively (Fig. 1). We investigated not only the three types of smartphones shown in this paper but also several additional models. We found that the antennas in many types of smartphones were installed in the lower part housing the smartphone. This has the effect of decreasing the SAR in the head during phone calls.

Therefore, in this study, we selected three antenna sizes and positions as typical models: "long to the left and right, lower center (model A)," "relatively small, lower left (model B)," and "relatively small, lower right (model C)." While these three models do not cover all cases, they do include almost all cases. Furthermore, they are relatively popular models with users.

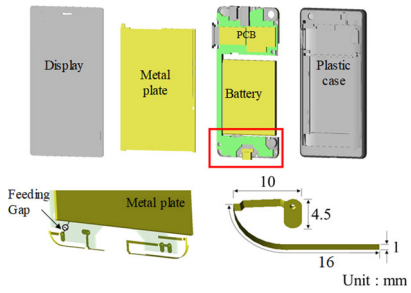

(a) Model A

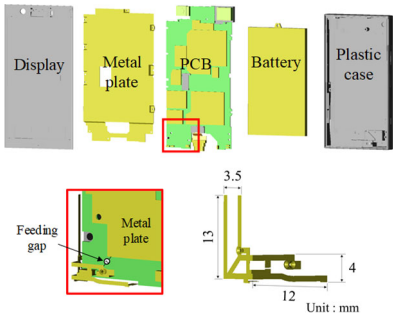

(b) Model B

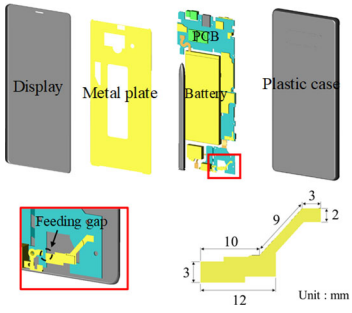

(c) Model C

Fig. 1 Developed smartphone models and enlarged view of each antenna.

Table 2 Reflection coefficients.

	Reflection coefficient (S_{11}) [dB]
Model A	-22
Model B	-14
Model C	-11

2.2 Validation of Developed Models

Three smartphone models were employed in this study based on 4th generation (4G) technology. The communication bands for the 4G system include some frequency bands. Each of the models used (smartphones A–C) covered different frequency bands. Among them, the 1950 MHz band was covered by all the models, which is also widely used in Japan. For these reasons, we investigated the characteristics of this frequency band.

The numerical smartphone model needs to satisfy several requirements: the antenna must work at the operating frequency (1950 MHz), and the model must reproduce an EM distribution in the near field of the actual smartphone. Table 2 shows the results of each reflection coefficient at the feeding point of the antenna in models A–C. The software used for the calculation was XFdtd, version 7.3 (Remcom Inc., Stage College, PA, USA) [10]. In these calculations, the minimum and maximum cell sizes were $0.2 \times 0.2 \times 0.2$ mm^3 and $1.0 \times 1.0 \times 1.0$ mm^3, respectively. The SAR calculations were performed after the EM wave in the calculation space became a steady state. We confirmed that, in all the models, the antenna worked at the operating frequency (1950 MHz), with the result that the reflection coefficient was lower than

−10 dB. Incidentally, when the abdomen of the human body model was close to the smartphone models (with the antenna models), the S_{11} values did not change significantly, because the hands and/or the head of the human body model did not adhere to the antenna.

In order to validate the EM radiation pattern and the local SAR of the smartphone model in the vicinity of the human body, we also compared the SAR measurements with the calculated values of the models. Figure 2 shows the measured and calculated results of the SAR distribution in the flat phantom when the display of the smartphone faced the phantom. The relative permittivity and conductivity of the phantom were 40 and 1.4 S/m, respectively. The electrical properties and positional relationship between the phantom and the smartphone were the same in the measurements and calculations. In the measurement, radiation power was controlled to the maximum power of an actual smartphone by a base station simulator (Anritsu, Kanagawa, Japan [12]), and the SARs were obtained by a cSAR3D (Schmid & Partner Engineering AG, Zurich, Switzerland [13]) in accordance with the International Electrotechnical Commission (IEC) 62209-3 [14]. The separation distance between the flat phantom and the smartphones was set to 0 mm. Such measurements are usually performed by setting the separation distance specified by the terminal manufacturer [1], [2]. However, since these measurements were only meant for model validation, the separation distance was set to 0 mm. Therefore, the SAR values shown in Fig. 2 exceeded the safety limits. In the calculation, radiation power was fixed at 0.2 W. In other word, the calculated SAR values were normalized by 0.2 W. In addition, 0.2 W is the maximum radiation power defined by the 4G standard [11].

In all the models, near the front of the antenna on the bottom right of the smartphone, the SAR values reached a maximum in both the measurement and calculation. As a result, the SAR distributions roughly matched in each calculation. The peak $SAR_{10\,g}$ calculations were 75–136% of the measurement results.

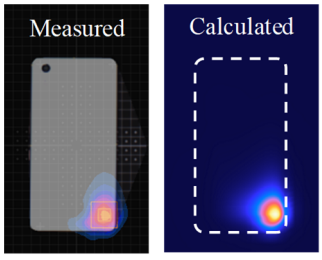

(a) Model A

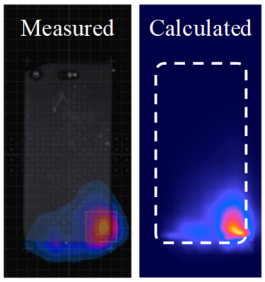

(b) Model B

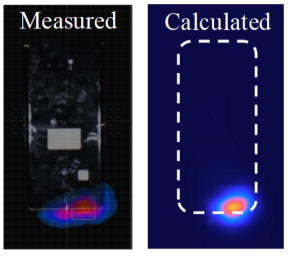

(c) Model C

Fig. 2 Measured and calculated SAR distributions.

3. SAR Calculations Using the Human Model

We calculated the $SAR_{10\,g}$ using the developed smartphone models and a high-resolution numerical human model (TARO) [15]. Figure 3 shows the calculation model. The minimum and maximum cell sizes in this calculation model were $0.2 \times 0.2 \times 0.2\,mm^3$ (for the smartphone model) and $2 \times 2 \times 2\,mm^3$ (for the human model and the surrounding), respectively. It is generally considered that 2 mm cells can be employed for a SAR calculation up to around 3 GHz. Therefore, these cell sizes were considered small enough for the study. The SAR calculations were performed after the EM wave in the calculation space became a steady state.

TARO is based on the realistic anatomical structure of a Japanese male and is composed of 51 types of tissue.

(a) Overall view

(b) Position of smartphone model

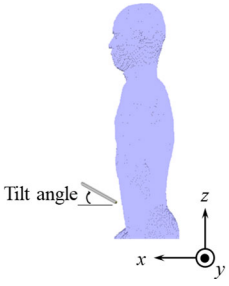

Fig. 3 Calculation model.

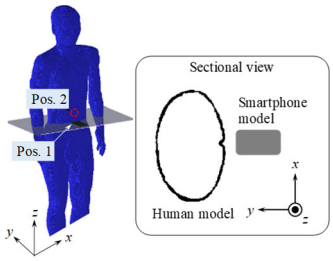

(a) Position 1

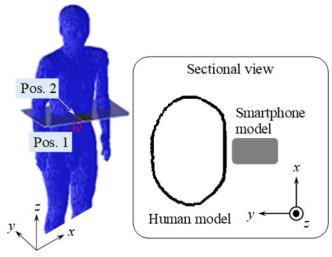

(b) Position 2

Fig. 4 Sectional view of positions 1 and 2.

The smartphone model was placed at the front of TARO's abdomen. It has been assumed that the smartphone was under the browsing position at the front of the abdomen, not the phone call. At this time, the hands for holding the smartphone were not considered. The SAR values in the body were considered to be higher under this condition. The distance between the surface of TARO and the surface of the smartphone was fixed at 15 mm. The distance may have been slightly small. However, these conditions were set in order to make worst-case evaluations while taking into account the actual usage styles. The operating frequency was 1950 MHz, and radiation power was fixed at 0.2 W, as in the previous descriptions. The tilt angle of the smartphone was changed in 5° increments. In calculation 1, the smartphone model was placed at the navel of the human model (position 1), a typical position for smartphones when held in front of the body. In calculation 2, the smartphone model was placed to the front but at a higher level than the navel (position 2). In position 1, there was concavity in the human body surface (Fig. 4). It was determined that position 2 did not have this level of concavity.

Figure 5 shows the peak $SAR_{10\,g}$ when the tilt angles of the smartphone changed in 5° increments. The tendencies of the SARs when the tilt angles were changed differed for each model. It was thought that this was caused by the difference in the antenna position of the smartphone. In models A and B, the SAR values increased as the tilt angle rose. This appeared to be because the distance between the antenna and the body surface decreased as the tilt angle rose. However, in model C, the SAR variations were smaller than those of the other two models. In order to analyze the fact, we considered the details of the model C structure, where the antenna was located a few mm inside from the bottom edge of the terminal case. As a result, the distance between the

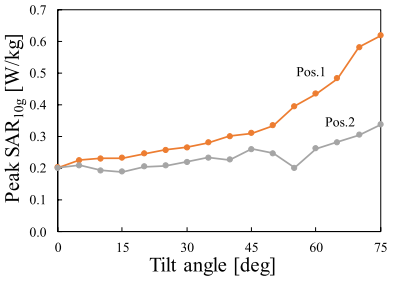

(a) Model A

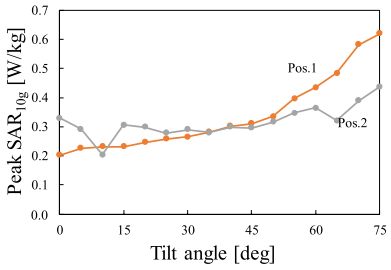

(b) Model B

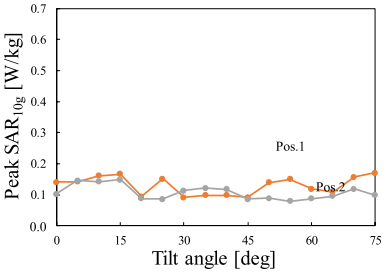

(c) Model C

Fig. 5 The peak $SAR_{10\,g}$ in the human model.

antenna and the human body surface was larger than in the other two models. Therefore, the variation in the distance did not increase, even if the tilt angle changed. As a result, the SAR variations were not very large in model C.

These results were summarized as a box plot in order to show the SAR variation due to angle fluctuation (Fig. 6). In the box plot, the central rectangles show quartiles, and the x mark in the rectangle represents the average. The lines under and above the rectangle represent minimum and maximum values, respectively. In the graphs, CV means coefficient of variation, which was calculated in order to evaluate the degrees of variation when the tilt angles of the smartphone were changed in each simulation. Based on the graph and each CV, there were larger SAR variations in position 1 than in position 2 in all the smartphone models. This might have been because the navel, the concavity on the surface of the human body, affects SAR variations. In other words, the closer to the flat surface, the smaller the SAR variation. Considering these results, we investigated the relationship between the SAR variation when the tilt angles of

the smartphone were changed and the surface of the human body affected variations in the SAR. In these calculations, we used a human model with uniform electrical properties in the whole body. Smartphone models were located at positions 1 and 2. In addition, at position 3, the SARs in the rectangular parallelepiped phantom (flat phantom) were calculated (Fig. 7). The relative permittivity and conductivity of the human model and flat phantom were 40 and 1.4 S/m, respectively. Figure 8 shows the SAR when the tilt angles of

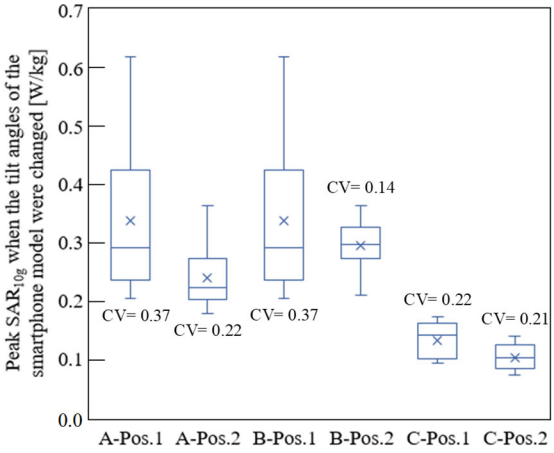

Fig. 6 SAR variation due to angle fluctuation.

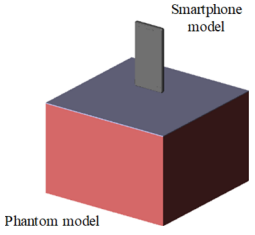

Fig. 7 Simulation model in position 3.

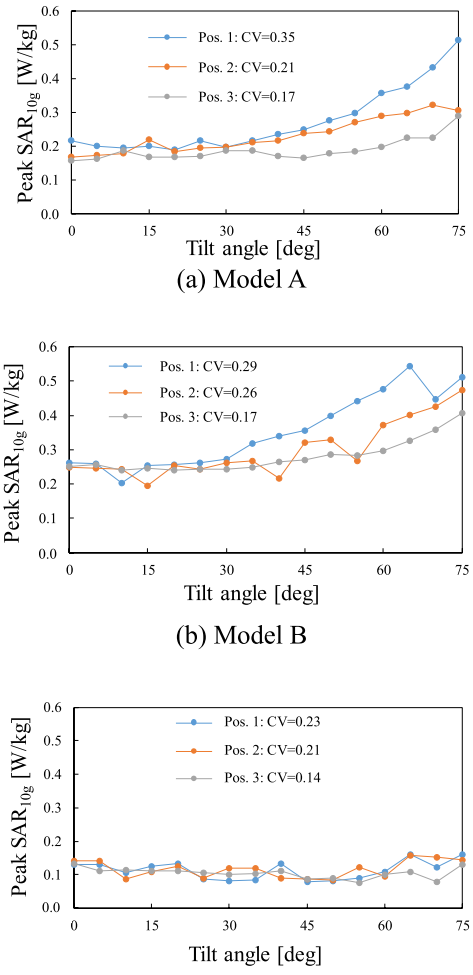

Fig. 8 The peak $SAR_{10\,g}$ in the human model, which has uniform electrical properties in the whole body (positions 1 and 2) and the flat phantom (position 3).

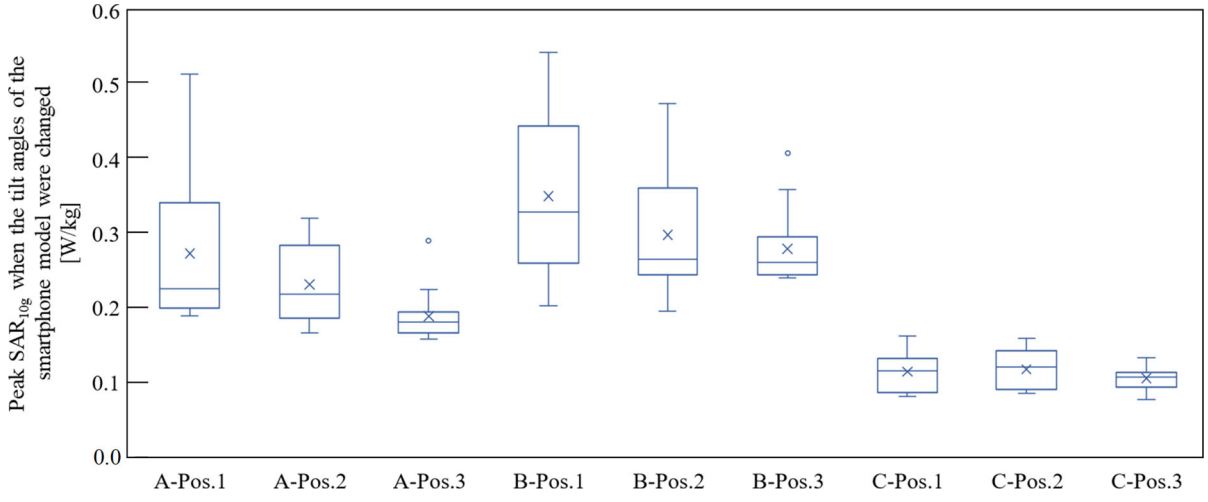

Fig. 9 SAR variation due to angle fluctuation in the human model, which has uniform electrical constants in the whole body (positions 1 and 2) and the flat phantom (position 3).

the smartphone models (A–C) were changed. In models A and B, when the tilt angles were increased, so did the peak $SAR_{10\,g}$. However, in model C, there were no significant changes in the peak $SAR_{10\,g}$ due to changes in the tilt angles of the smartphone. These were the same tendencies as those in the aforementioned simulations using TARO. Figure 9 shows SAR variations due to angle fluctuation. In all the smartphone models, the CV reached a maximum in position 1, followed by positions 2 and 3. These results show that if the surface is flat and smooth, the SAR variation tends to be smaller. Therefore, in the human body, the SAR variation due to changes in the tilt angle of the smartphone is considered to be larger than in the flat phantom because the human body surface has a curved surface and is uneven. Furthermore, the heterogeneity of the electrical properties in the human model was not as important to the SAR variations.

4. Conclusion

In this study, we developed high-resolution numerical smartphone models based on actual smartphones and calculated SARs in the human body using a smartphone at various tilt angles. The tendencies of the SARs when the tilt angles changed differed for each smartphone model. In addition, from the CV results, the SAR variations appeared to be related to the surface shape of the human body rather than the electrical properties of the human model. Therefore, the SAR variations in real human bodies are larger than those of the flat phantom. However, these results depend on the frequency and would benefit from further study.

Acknowledgments

Part of this work was supported by the Ministry of Internal Affairs and Communications, Grant Number JPMI10001.

References

[1] ICNIRP, "Guidelines for limiting exposure to electromagnetic fields (100 Hz to 300 GHz)," Health Phys., vol.118, no.5, pp.483–524, 2020.
[2] IEEE Standard for Safety levels with Respect to Human Exposure to Radio Frequency Electromagnetic fields, 3 kHz to 300 GHz IEEE Standard C95. 1-2005, 2005.
[3] V. Hombach, K. Meir, M. Burkhardt, E. Kuhn, and N. Kuster, "The dependence of EM energy absorption upon human head modeling at 900 MHz," IEEE Trans. Microw. Theory Techn., vol.44, no.10, pp.1865–1873, Oct. 1996.
[4] A.D. Tinniswood, C.M. Furse, and O.P. Gandhi, "Computations of SAR distributions for two anatomically based models of the human headusing CAD files of commercial telephones and the parallelized FDTD code," IEEE Trans. Antennas Propag., vol.46, no.6, pp.829–833, June 1998.
[5] P. Bernardi, M. Cavagnaro, S. Pisa, and E. Piuzzi, "A graded-mesh FDTD code for the study of human exposure to cellular phones equipped with helical antennas," Appl. Comput. Electromagn. Soc. J., vol.16, no.2, pp.90–96, 2001.
[6] S. Pisa, M. Cavagnaro, V. Lopresto, E. Piuzzi, G.A. Lovisolo, and P. Bernardi, "A procedure to develop realistic numerical models of cellular phones for an accurate evaluation of SAR distribution in the human head," IEEE Trans. Microw. Theory Techn., vol.53, no.4, pp.1256–1265, April 2005.
[7] B. Xu, M. Gustafsson, S. Shi, K. Zhao, Z. Ying, and S. He, "Radio frequency exposure compliance of multiple antennas for cellular equipment based on semidefinite relaxation," IEEE Trans. Electromagn. Compat., vol.61, no.2, pp.327–336, 2019.
[8] A. Tateno, K. Tanaka, T. Nagaoka, K. Saito, S. Watanabe, M. Takahashi, and K. Ito, "Comparison of SAR in human body radiated from mobile phone and tablet computer," Proc. Int. Symp. EMC, Tokyo, Japan, pp.186–189, May 2014.
[9] R. Takei, T. Nagaoka, K. Saito, S. Watanabe, and M. Takahashi, "SAR variation due to exposure from a smartphone held at various positions near the torso," IEEE Trans. Electromagn. Compat., vol.59, no.2, pp.747–753, April 2017.
[10] Remcom Inc., State College, PA, USA, "3D EM simulation — FDTD simulation software XFdtd — remcom," https://ja.remcom.com/xfdtd-3d-em-simulation-software
[11] 3rd Generation Partnership (3GPP), "Technical specification group radio access network; User equipment (UE) radio transmission reception (FDD)," TS 25.101.
[12] Anritsu, Kanagawa, Japan, https://www.anritsu.com/ja-jp
[13] SPEAG, Zurich, Switzerland, https://speag.swiss/
[14] IEC 62209-3:2019 Measurement procedure for the assessment of specific absorption rate of human exposure to radio frequency fields from hand-held and body-mounted wireless communication devices - Part 3: Vector measurement-based systems (Frequency range of 600 MHz to 6 GHz), 2019.
[15] T. Nagaoka, S. Watanabe, K. Sakurai, E. Kunieda, S. Watanabe, M. Taki, and Y. Yamanaka, "Development of realistic high resolution whole-body voxel models of Japanese adult male and female of average height and weight, and application of models to radio-frequency electromagnetic-field dosimetry," Phys. Med. Biol., vol.49, no.1, pp.1–15, 2004.

Chiaki Takasaka received the B.E. and M.E. degree in 2019 and 2021, respectively from Chiba University, Chiba, Japan. She is currently working with Canon Electron Tubes & Devices, Tochigi, Japan. Her main interest is the evaluation of the interaction between the electromagnetic field and the human body.

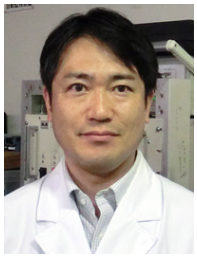

Kazuyuki Saito was born in Nagano, Japan, in May 1973. He received the B.E., M.E. and Ph.D. degrees all in electronic engineering from Chiba University, Chiba, Japan, in 1996, 1998 and 2001, respectively. He is currently an Associate Professor with the Center for Frontier Medical Engineering, Chiba University. His main interest is in the area of medical applications of the microwaves including the microwave hyperthermia. He received the IEICE AP-S Freshman Award, the Award for Young Scientist of URSI General Assembly, the IEEE AP-S Japan Chapter Young Engineer Award, the Young Researchers' Award of IEICE, and the International Symposium on Antennas and Propagation (ISAP) Paper Award in 1997, 1999, 2000, 2004, and 2005 respectively. Dr. Saito is a Senior member of the Institute of Electrical and Electronics Engineers (IEEE), member of the Institute of Image Information and Television Engineers of Japan (ITE), the Japanese Society for Thermal Medicine (JSTM), and the Japan Society for Endoscopic Surgery (JSES).

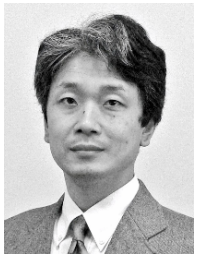

Masaharu Takahashi was born in Chiba, Japan, in December 1965. He received the B.E. degree in electrical engineering in 1989 from Tohoku University, Miyagi, Japan, and the M.E. and D.E. degree in electrical engineering from Tokyo Institute of Technology, Tokyo, Japan, in 1991 and 1994, respectively. He was a Research Associate from 1994 to 1996, an Assistant Professor from 1996 to 2000 at Musashi Institute of Technology, Tokyo, Japan, and an Associate Professor from 2000 to 2004 at Tokyo University of Agriculture & Technology, Tokyo, Japan. He is currently an Associate Professor at Chiba University, Chiba, Japan. He served as Editor-in-Chief of IEICE Transactions on Comminication from 2011 to 2013, Vice Chair of Editorial Board, IEICE Communication Society from 2013 to 2014, Editor in chief of Editorial committee of IEICE Communications Society Magazine (Japanese Edition) from 2014 to 2016, Chair of Technical Committee on Wireless Power Transfer, IEICE from 2018 to 2020, Vice President of IEICE-CS Board from 2019 to 2021, Chair of Planning and Member Activities Committee, IEICE-CS from 2019 to 2021, and Chair of IEEE Antennas & Propagation Society Tokyo Chapter from 2019 to 2020. His main interests have been electrically small antennas, RFID, Implanted antennas, EMC and research on evaluation of the interaction between electromagnetic fields and the human body by use of numerical and experimental phantoms. He is a Fellow of IEICE and a Senior member of IEEE.

Tomoaki Nagaoka received the Ph.D. degree in medical science from Kitasato University, Kanagawa, Japan, in 2004. He is currently a Senior Researcher with the Electromagnetic Compatibility Laboratory, Applied Electromagnetic Research Institute, National Institute of Information and Communications Technology, Tokyo, Japan. His main research interests include biomedical electromagnetic compatibility and medical image analysis. Dr. Nagaoka is a Member of the IEEE Microwave Theory and Techniques Society and the Institute of Electronics, Information and Communication Engineers, Japan. He received several awards, including the 2004 Best Paper Award in Physics in Medicine and Biology, the 2007 Young Researcher Award from the IEICE, the 2008 International Scientific Radio Union Young Scientist Award, the 2011 Outstanding Paper Award from IEEE AFRICON, and the 2011 Best Paper Award from ISABEL'11.

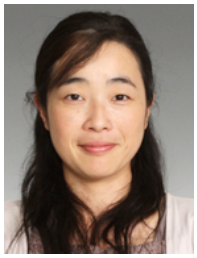

Kanako Wake received the Ph.D. degree in medical science from Tokyo Metropolitan University, Tokyo, Japan, in 2000. In the same year, she joined the Ministry of Posts and Telecommunications Communications Research Laboratory (currently the National Institute of Information and Communications Technology). Her main research interests include biomedical electromagnetic compatibility and she is currently the research manager of the Electromagnetic Environment Laboratory, Electromagnetic Research Institute. Dr. WAKE is a member of the Institute of Electronics, Information and Communication Engineers of Japan, the IEEE Bioelectromagnetics Society.